Marine Technology, Vol. 42, No. 3, October 2005, pp. 159–176

Numerical Simulation of Ship Maneuverability in Wind and Current, With Escort Tugs

Ye Li[1] and **Sander M. Çalışal**[1]

A number of recent large-ship accidents have compelled naval architects and engineers to advance the research on ship maneuverability and the prediction of ship response in the ocean environment. In the meantime, new maneuverability standards have been developed and the International Maritime Organization (IMO) has also proposed one such standard. This standard provides four ship-maneuvering performance criteria, and its latest version is dated December 2002. Simulation technology, in particular the simulation of ship maneuvering, has advanced considerably in recent years with the advent of computers. Computer programs using either numerically computed or experimentally determined hydrodynamics coefficients have allowed an accurate simulation of ship maneuverability for different types of vessels. Relatively good agreement has been reported by various researchers between simulated results and those obtained from full-scale ship trials. It seems that simulation can now identify acceptable ship maneuvering performance in calm seas. However, the effects of wind and current and escort tug assistance have not been that well studied and reported, and they are always important factors for ship maneuvering especially in restricted waters. The numerical simulation program presented in this paper (UBCManeuver) has been validated using data on the *Esso Osaka* 278,000 DWT tanker, a ship well tested for regular maneuvering tests. UBCManeuver is able to identify IMO class and non-IMO class ships according to the most recent IMO standards for ship maneuverability. A good agreement was obtained between simulation and the sea trials reported for *Esso Osaka*. After the validation of the code, the course-keeping abilities of this ship in restricted waters were studied in calm seas and under wind and current conditions. The effect of escort tugs on such an operation has also been quantified and *Esso Osaka's* maneuvering performance around Vancouver harbor simulated. The limits of current and wind strengths for "successful" operation with and without escort tugs have then been established. In addition, the effectiveness of multiple tug assistance in different positions is discussed in some detail.

Introduction

DURING THE LAST FOUR DECADES, ship size, especially tanker size, has increased continuously. Various tanker accidents have been well reported by the media, as they usually cause extensive environmental damage. Many disasters have happened around touristic coastal areas in France and Spain, or in environmentally sensitive areas, such as Alaska. Because of the environmental risk, ship safety and especially tanker safety have become a major concern. As a result, many organizations and government offices around the world have become involved in ship safety (Crane 1973, Eda et al 1979, Doerffer 1980, Palomares 1994). In the United States, the federal government passed the Ports and Waterways Safety Act in 1971 and the Ports and Tanker Safety Act in 1978. After the accidents of the *Torey Canyon* in 1967 and the *Amoco Cadiz* in 1978, the public and technical concerns increased and significant research on ship safety has followed. In particular, the International Maritime Organization (IMO) developed new ship standards for ship maneuverability, which are now accepted and used by a large number of countries while some individual countries have their own specific criteria. In this paper, we will use the current version of IMO standards as the main criteria for ship maneuvering.

[1] Naval Architecture Lab, Department of Mechanical Engineering, University of British Columbia, Vancouver, British Columbia, Canada.

Manuscript received at SNAME headquarters July 2004.

Numerical ship simulation is now well developed and is a very useful design tool for naval architects. The IMO Standards for Ship Maneuverability and its explanations were finalized in 2002 (MSC 76), and its explanation was slightly modified in 2004 (DE 47). In this paper these IMO requirements were used to identify IMO class and/or non-IMO class ships by simulation. In addition, we investigated tanker maneuvering in the presence of current and wind forces in order to quantify the importance of these forces on ship maneuvering and course keeping near entrances to harbors.

A tanker well known from many ship maneuvering studies, the *Esso Osaka* 278,000 DWT was selected as the objective test vessel, and the Vancouver Harbor (Fig. 1) was used for the definition of maximum wave and wind conditions and coastal navigation geometry. The safe entrance to the Vancouver Harbor under various combinations of external forces was then studied. The effect of escort tugs on ship maneuvering and on IMO requirements was then quantified.

IMO Standards for ship maneuverability

Since 1971, IMO has published recommendations for rudder size, mainly for ship maneuverability and ship safety. Statistically, in the 1970s there were about 200 shipwrecks per year and in total 1,200,000 DWT corresponding to about 0.4% of the world ship displacement, that is, about 50,000 DWT was lost every 2 weeks. The prime causes of these losses, about 48% of the total wreck DWT, were collision and grounding, and most of them originated in maneuvering problems (Baquero 1982). IMO established special sub-

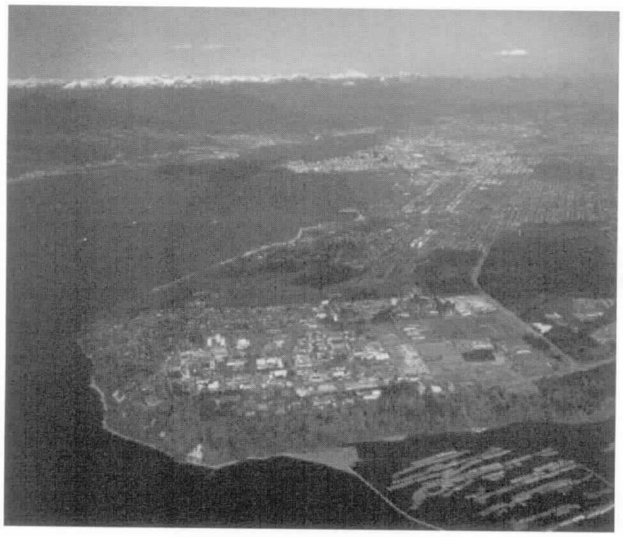

Fig. 1 Aerial view of the approach to Vancouver Harbor

organizations for ship maneuvering studies, such as the Maritime Safety Committee (MSC), the subcommittee Design and Equipment (DE), and the Working Group (WG).

At MSC 76, the Maritime Safety Committee adopted the current version of the Standards for Ship Maneuverability (Resolution MSC 136 [76]) on December 4, 2002. The MSC also adopted a new set of Explanatory Notes to the Standards for Ship Maneuverability (MSC/Circ. 1053), although there were some changes in DE 47 in March 2004. These new standards now supercede the original Interim Standards and Explanatory Notes (MSC/Circ. 644). Designers and researchers wrote their understanding and expressed their concerns on the IMO Standard for Ship Maneuverability. A summary work by Daidola et al (2002) concerning MSC/Circ. 644 and ship maneuvering prediction by Gray et al (2003) are worth noting. Simulations and sea trials, according to the Interim Standards for Ship Maneuverability, were well reported by Hasegawa and Sasaki (1997) and Guedes Soares et al (2004).

The current IMO Standard for Ship Maneuverability given in MSC/Circ. 1053 can be summarized as containing four distinct criteria:

1. Turning ability. The requirement is that the advance should not exceed 4.5 times the ship length (L) and the tactical diameter should not exceed 5 times the ship length in a turning circle maneuver.
2. Initial turning ability. In a zigzag maneuvering, the ship should not travel more than 2.5 times the ship length by the time the heading has changed by 10 deg from the original heading after the application of 10 deg rudder to port/starboard.
3. Yaw-checking and course-keeping abilities. The value of the first overshoot angle in the 10 deg/10 deg zigzag test should not exceed
   - 10 deg if L/V is less than 10 s
   - 20 deg if L/V is 30 s or more
   - 5.5 (L/V) deg if L/V is 10 s or more, but less than 30 s, where L and V are expressed in m and m/s, respectively.

   The value of the second overshoot angle in the 10 deg/10 deg zigzag test should not exceed

   - 25 deg, if L/V is less than 10 s
   - 40 deg, if L/V is 30 s or more

   [17.5 + 0.75(L/V)] deg, if L/V is 10 s or more, but less than 30 s.

   The value of the first overshoot angle in the 20 deg/20 deg zigzag test should not exceed 25 deg.
4. Stopping ability. This test requires that the track reach in the full astern stopping test should not exceed 15 times the ship length. However, this value may be modified where ships of large displacement make this criterion impracticable, but as an upper limit, it should in no case exceed 20 ship lengths.

Mathematical model

General

Ship simulation has been recognized as a valuable design and decision-making tool for predicting ship performance, and various studies have been published in past years. The control model selected for this study is the *Esso Osaka* 278,000 DWT without external effects. The particulars are as reported by ITTC 1978, and the data used for validation are from Kim (1988) of Korean Research Institute of Ship and Ocean (KRISO). The equations used are given below:

$$\left.\begin{aligned}
m(\dot{u} - \nu r - x_G r^2) &= X_{\dot{u}}\dot{u} + X_{\nu r}\nu r + [X_{\nu\nu} + X_{\nu\nu\eta}(\eta - 1)]\nu^2 \\
&\quad + [X_{rr} + X_{rr\eta}(\eta - 1)]r^2 \\
&\quad + [X_{\delta\delta} + X_{\delta\delta\eta}(\eta - 1)]\delta^2 \\
&\quad - (\text{Resistance}) + (\text{Thrust}) \\
m(\dot{\nu} + ur + x_G\dot{r}) &= Y_o + Y_{o\eta}(\eta - 1) + Y_{\dot{\nu}}\dot{\nu} + Y_{\dot{r}}\dot{r} \\
&\quad + [Y_\nu + Y_{\nu\eta}(\eta - 1)]\nu + [Y_r + Y_{r\eta}(\eta - 1)]r \\
&\quad + [Y_{\nu|\nu|} + Y_{\nu|\nu|\eta}(\eta - 1)]\nu|\nu| \\
&\quad + [Y_{r|r|} + Y_{r|r|\eta}(\eta - 1)]r|r| + Y_{\nu rr}\nu r^2 \\
&\quad + Y_{r|v|}r|v| \\
&\quad + [Y_\delta + Y_{\delta\eta}(\eta - 1)]\delta + Y_{\delta|\delta|}\delta|\delta| \\
&\quad + Y_{\delta\nu\nu}\delta\nu^2 \\
I_z\dot{r} + mx_G(\dot{\nu} + ur) &= N_o + N_{o\eta}(\eta - 1) + N_{\dot{\nu}}\dot{\nu} + N_{\dot{r}}\dot{r} \\
&\quad + [N_\nu + N_{\nu\eta}(\eta - 1)]\nu + [N_r + N_{r\eta}(\eta - 1)]r \\
&\quad + [N_{\nu|\nu|} + N_{\nu|\nu|\eta}(\eta - 1)]\nu|\nu| \\
&\quad + [N_{r|r|} + N_{r|r|\eta}(\eta - 1)]r|r| + N_{\nu rr}\nu r^2 \\
&\quad + N_{r|\nu|}r|\nu| \\
&\quad + [N_\delta + N_{\delta\eta}(\eta - 1)]\delta + N_{\delta|\delta|}\delta|\delta| \\
&\quad + N_{\delta\nu\nu}\delta\nu^2
\end{aligned}\right\} \tag{1}$$

where resistance and thrust in the first equation of equations (1) are the values obtained from towing tank resistance tests and the propeller thrust is obtained from open water and self-propulsion tests. Please refer to Kim (1988) for representation of the propulsive system dynamics. To compensate for the propeller side force that is not available from tank tests, in stopping maneuvering, an initial disturbance of 2.5 deg in heading angle is introduced only in the simulation of stopping.

The effect of wind and current

Wind and current are both important external effects on a ship. While retaining the left-hand side (LHS) of equation (1), the right-hand side (RHS) of the general governing equation with wind and current effects can be modified as follows:

$$\left.\begin{aligned}
\text{RHS}(1) &= X + X_C + X_{Wd} \\
\text{RHS}(2) &= Y + Y_C + Y_{Wd} \\
\text{RHS}(3) &= N + N_C + N_{Wd}
\end{aligned}\right\} \tag{2}$$

where X_C, Y_C, and N_C refer to the current forces in the x and y directions and the yaw moment, X_{Wd}, Y_{Wd}, and N_{Wd} refer to the wind-caused forces and moment. The terms X, Y, and N refer to the remaining terms on the right-hand side of equation (1).

Generally, wind and current force model is an experimentally and statistically determined algorithm. There are many alternative ways to calculate these forces, such as Van Berlekon et al (1974) and Wagner (1967). One such algorithm, published by The Oil Companies International Marine Forum (OCIMF 1977), was selected for the calculation of these terms. The OCIMF model is considered to be one of the better suitable algorithms for tanker studies, as this algorithm focuses on very large crude carrier (VLCC), tanker, and floating production, storage, and offloading (FPSO) shapes. The OCIMF model expresses the wind and current forces as follows:

$$\left.\begin{aligned} X_{Wd} &= C_{Xwd} \times \left(\frac{\rho_{Wd}}{7{,}600}\right) \times V_{Wd}^2 \times A_T \\ Y_{Wd} &= C_{Ywd} \times \left(\frac{\rho_{Wd}}{7{,}600}\right) \times V_{Wd}^2 \times A_L \\ N_{Wd} &= C_{Nwd} \times \left(\frac{\rho_{Wd}}{7{,}600}\right) \times V_{Wd}^2 \times A_L \times L_{BP} \end{aligned}\right\} \quad (3)$$

$$\left.\begin{aligned} X_C &= C_{Xc} \times \left(\frac{\rho_C}{7{,}600}\right) \times V_C^2 \times A_T \\ Y_C &= C_{Yc} \times \left(\frac{\rho_C}{7{,}600}\right) \times V_C^2 \times A_L \\ N_C &= C_{Nc} \times \left(\frac{\rho_C}{7{,}600}\right) \times V_C^2 \times A_L \times L_{BP} \end{aligned}\right\} \quad (4)$$

Equation (3) is given for wind forces, and equation (4) is used for current forces and moment.

Tug assistance

As ships have become larger and larger in recent years, and as tankers have been built larger and are required to deliver their payloads faster, a greater demand has been placed on the performance of the tugs that assist them. This is especially true in coastal areas where ship system failure or human error, such as wrong maneuvering, can lead to more severe nautical disasters, such as grounding or collision, and may result in devastating environmental damage. A specialized class of tugs, escort tugs, has been developed to assist larger ships in maneuvering or mooring, as shown in Fig. 2.

The tug employed in this simulation study is a variation of an escort tug designed by Robert Allen Ltd. and tested at the Institute of Marine Dynamics (IMD). The data were obtained and analyzed by Ratcliff (2004).

Fig. 2 Escort tug assistance

Tugs can provide a breaking and steering force for ships. The forces generated by an escort tug linked to a tanker are shown in Fig. 3. The mathematical model for the tug-generated forces and the environmental forces are given in equations (5) to (8).

$$\left.\begin{aligned} \mathrm{RHS}(1) &= X + X_e \\ \mathrm{RHS}(2) &= Y + Y_e \\ \mathrm{RHS}(3) &= N + N_e \end{aligned}\right\} \quad (5)$$

$$X_e = \begin{cases} 0 & F_{Sm} \geq (X_C + X_{Wd}) \\ X_C + X_{Wd} - F_{Sm} & F_{Sm} < (X_C + X_{Wd}) \end{cases} \quad (6)$$

$$Y_e = \begin{cases} 0 & F_{Bm} \geq (Y_C + Y_{Wd}) \\ Y_C + Y_{Wd} - F_{Bm} & F_{Bm} < (Y_C + Y_{Wd}) \end{cases} \quad (7)$$

$$N_e = \begin{cases} 0 & N_{Tm} \geq (N_{Wd} + N_C) \\ N_{Wd} + N_C - N_{Tm} & N_{Tm} < (N_{Wd} + N_C) \end{cases} \quad (8)$$

where X_e, Y_e, and N_e denote the external environmental forces and moment, and F_{Sm}, F_{Bm}, and N_{Tm} denote the maximum steering force, the breaking force, and the yaw moment the escort tug can provide.

Even without environmental forces, an escort tug can provide appropriate maneuvering forces and moments. Therefore, the general mathematical model for tug assistance can be rewritten as in equation (9):

$$\left.\begin{aligned} \mathrm{RHS}(1) &= X + X_C + X_{Wd} - F_S \\ \mathrm{RHS}(2) &= Y + Y_C + Y_{Wd} - F_B \\ \mathrm{RHS}(3) &= N + N_C + N_{Wd} - N_T \end{aligned}\right\} \quad (9)$$

where F_S, F_B, and N_T denote the steering force, breaking force, and the moment an escort tug can provide. In addition, the mathematical model for an escort tug connected at the bow of the tanker is the same as for one connected at the stern while the forces and moment values are somewhat smaller.

Shallow water effect

The *Esso Osaka* 278,000 DWT is a well-studied tanker, which underwent trials in a relatively shallow water area (Crane 1979a, 1979b). Shallow water effects could be included in mathematical modelings. The studies reported in the literature, such as the one by the Seoul National University (SNU) and by the Hydronautics, Inc., Ship Model Basin (HSMB) and the model recommended by the Specialist committee of ITTC (2002) for *Esso Osaka* models, did not consider the finite water effects. As validation is a comparison between numerical simulation and sea trials, and the sea trials were in finite or shallow water areas, the shallow water effects have to be considered.

Mathematically, taking the sway term as an example, the right-hand side of the governing equation should contain

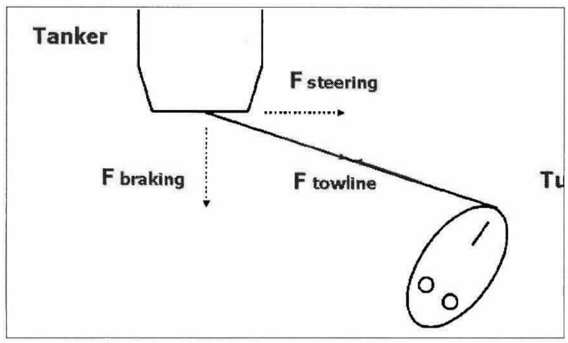

Fig. 3 Escort tug force model

terms with derivatives with respect to z, such as terms $Y_m r^2 z$ or the hydrodynamic coefficients used in the simulation should depend on depth. As none of the formulations has terms to represent finite water effects, one could consider adding additional terms on the right-hand side of the equation to represent finite water effects.

The procedure used in this study is to combine the finite water problem with the current force model, that is, to use the current effect term to represent both the current effect and the shallow water effects. This is done as follows:

$$Y_C = f(V_C, C_{Yc}) \tag{10}$$

$$C_{Yc} = g(H/D) \tag{11}$$

where V_C, H, and D denote current speed, water depth, and ship draft.

As was referred to above, the effect of current strongly depends on the water depth, especially in shallow water areas. Therefore, a quasi-zero speed current condition is used to approximate the calm, shallow water effects.

Mathematically, in this study, three items were added to the right-hand side of the equation (1), which are

$$\left.\begin{array}{l} X = f_1(V_C, C_{Xc}) \\ Y = f_2(V_C, C_{Yc}) \\ N = f_3(V_C, C_{Nc}) \end{array}\right\} \tag{12}$$

where $V_C \to 0$, that is, the values at zero speed are taken to be the shallow water effect. An external force of shallow water effect on the right-hand side of the governing equation is included for this purpose. This term is taken and revised from OCIMF (1977). For instance,

$$\left. Y_S = C_{Y_S} \times \left(\frac{\rho_W}{7{,}600}\right) \times V_W^2 \times A_L \right\}$$

where Y_S denotes the shallow water effect in the Y axis, $C_{Y_S} = g(H/D)$.

In fact, as in real sea trials in which one expects to have some wave and current effect, this formulation can be considered to be more realistic.

Course keeping

The course-keeping problem is another important issue in ship maneuvering. In this study, rudder control has been used for course keeping. The rudder response equation used in this paper is from Nomoto et al (1957) and can be written as follows

$$T\dot{r} + r = K\delta \tag{13}$$

where K and T denote the coefficients of Nomoto's equation, r denotes the yaw speed, and δ denotes the rudder angle.

There are various strategies commonly applied in ship control problems, such as robust control, fuzzy control, and neural network application. They are all very advanced and suitable strategies based on general control theory. Some very successful applications in this area of ship simulation have been reported by Djouani and Hamam (1996) and Kvam et al (2000). The proportional integral derivative (PID) control algorithm employed in this study together with the Nomoto equation is as follows:

$$\delta = K_P\left((\psi_d - \psi) + \frac{1}{sT_i}(\psi_d - \psi) + T_d\,(\dot{\psi}_d - \dot{\psi}) \right) + \frac{T}{K}\ddot{\psi} + \frac{1}{K}\dot{\psi} \tag{14}$$

where K_p, T_i, and T_d denote the P, I, and D coefficients in PID control. ψ_d denotes the desired heading angle.

The entire control system architecture is given in Fig. 4.

Simulation and sea trial

Simulation with UBCManeuver

In order to fully examine and verify the mathematical model of a given marine vehicle, it is necessary to compare the predictions based on a simulation program with the experimental data. In this study, the ship maneuvering and course-keeping simulation was formulated in time domain. Using *Esso Osaka* as an example, the governing equations, equation (1), equation (2), and/or equation (5), were used and integrated in time domain. The variables were obtained and modified in time domain. In the core part of UBCManeuver, the governing equation, that is, equation (1), combined with the external effects model have been coded as one file. To do this, we used the simulation software MATLAB from Mathworks, Inc. All of the IMO standards tests have been obtained by accessing this core file as a function. The numerical simulation was then validated using published and experimental data. The outputs of the simulation are the IMO test results as listed above. The ship-specific data were in a separate input file, and the test requirements were in other files. This allowed a flexible procedure whereby one can change the ship input file when a new simulation is done on a ship.

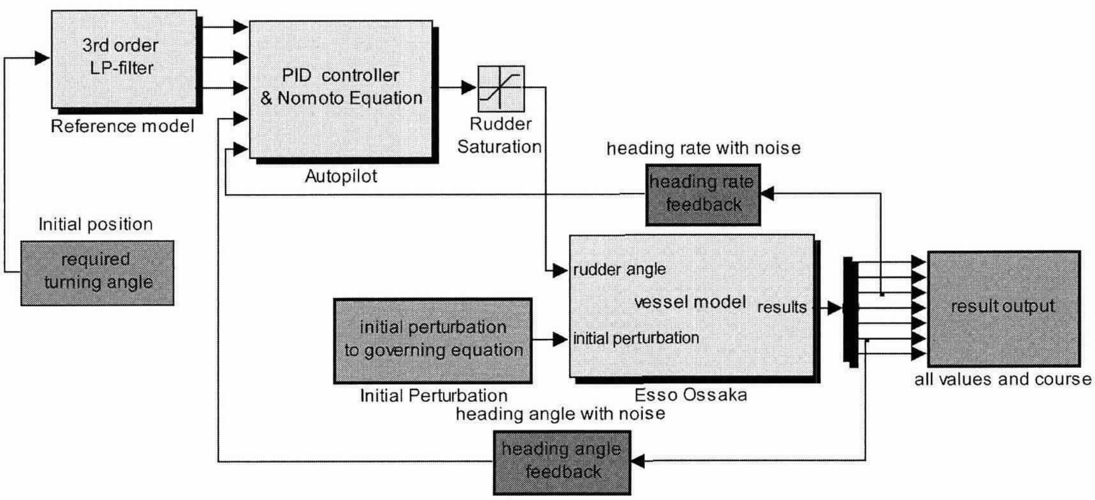

Fig. 4 Control system architecture

The course-keeping simulations were done using Simulink, also from Mathworks, Inc. For the simulation system discussed above, there are some special parameters that should be set in the control loop and marine vehicle model *Esso Osaka*. These parameters were obtained by tuning, by following guidelines and/or statistical database. In this study they have been expressed as follows:

1. For the control system, the PID controller was employed. The P, I, and D parameters K_p, T_i, and T_d for the PID controller are taken to be 10, 50, and 1,000 after tuning.
2. Both heading rate and heading angle feedback with noise in Fig. 4 are set as 1 for the control system, which indicates that there is no noise.
3. For the first-order Nomoto equation, equation (13) of the *Esso Osaka*, K and T are given as 0.0185 and 110.

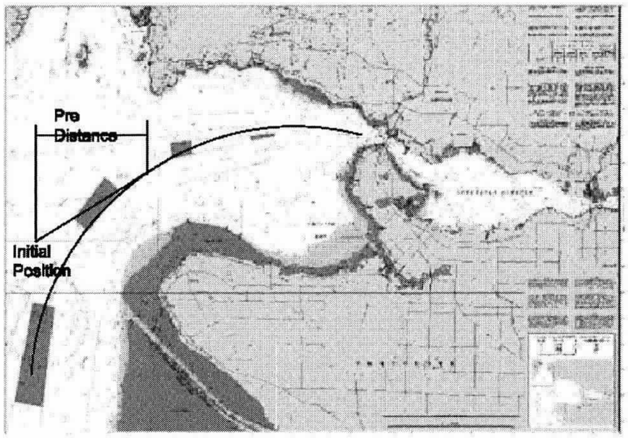

Fig. 5 Entrance strategy

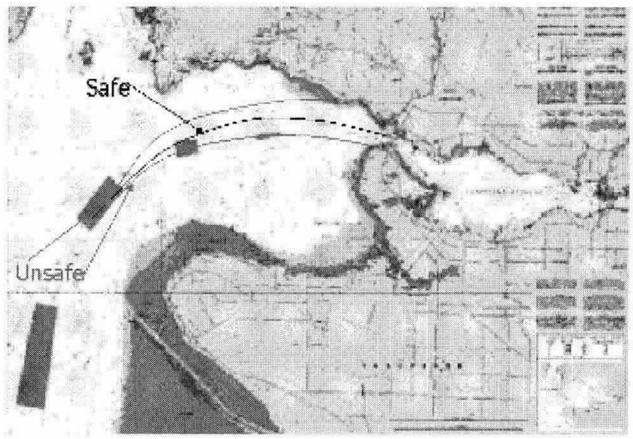

Fig. 6 Safe and unsafe operation definition

Sea trial and validation of UBCManeuver

The simulation program UBCManeuver was validated using sea trial results of *Esso Osaka* 278,000 DWT. One of the series of sea trials was made in shallow water (20% and 50% bottom clearance), and the other series of tests were conducted in deep water (more than 320%) in the Gulf of Mexico in July and August 1977. The sea trials were cooperative efforts of the US government and the American Institute of Merchant Shipping and were conducted by Exxon International. The details of the test conditions, information about the tests, and the results were reported by Crane (1979a, 1979b). However, only the wind conditions were well reported, and the current conditions were not reported. This might cause some differences between the simulation and sea trial results.

Several maneuvering tests, such as turning circle, zigzag maneuver, stopping, coasting turning circle, and coasting zigzag maneuver, were done. These trials addressed the effects of water depth, ship speed, and propeller RPM. All these tests can be simulated by the program UBCManeuver. Nevertheless, trials with numerical results were selected for validation purposes. The graphical results are given in Figs. 7 and 8.

Entrance to harbor

As most nautical disasters happen near harbors or coastal areas, the course-keeping potential of a ship, especially safe entrance into harbors, is important. Problems concerning course keeping have been studied by many researchers in the past few years (e.g., Webb & Hewlett 1992, Gray et al 2003). Vancouver Harbor has been taken here as an example for study purposes primarily because we were able to collect data about it. Vancouver Harbor is one of the biggest and busiest ports in Canada and the Pacific Rim. Every year, more than 3,000 ships from all over the world and numerous yachts pass by or dock here. As the tidal currents and wind conditions can be significant at the entrance to the harbor, First Narrows, we decided to simulate and investigate a ship's navigational and maneuvering performance specifically around the Vancouver Harbor.

The ship was controlled to sail directly into the harbor using the dedicated navigational channel. After she reached an appropriate distance, she was instructed to turn her heading angle. Finally, she was expected to enter into the harbor/channel successfully in a straight course, as shown in Fig. 5. This is defined as the safe entrance. However, under some weather and current conditions, the vessel was observed not to turn successfully at the proper heading angle as required. Therefore, the ship was judged not able to enter into the harbor successfully, which is defined as unsafe entrance, as shown in Fig. 6. This condition has been labeled as the unsafe condition for the wind and current strengths used in the simulation.

Table 1 Enforce condition

Wind effects	11.9 knots (−15 deg)
Tanker speed	7.2 knots
Propeller	39 RPM as constant
Tanker rudder	−34 deg

Numerical simulation results analysis

Program validation UBCManeuver

1. As stated, the program was validated using data reported from the sea trials for *Esso Osaka*. The trial conditions applied are listed in Table 1. The tactical diameter obtained under these conditions was 1,564 m. This value was obtained from Fig. 7*a*. The simulation results were then compared with the experimental tactical diameter reported by Crane (1979a, 1979b), as shown in Fig. 7*b*, which is 1,591 meters. The difference between these numbers is 1.7%. One can claim that a good agreement has been obtained between the results of simulation done by UBCManeuver and the full-scale experimental results. During the simulation, the initial ship speed is selected according to the MSC 1053 as around 85% of the ship power, which gives a ship speed of 15 knots. The time history of the propeller RPM is as follows: At the time the "full astern stopping" starts, the propeller RPM is changed to full astern at 70 RPM and remains at this value

until the ship stops. As in the simulation model, there is no propeller side force; an initial disturbance of heading angle by 2.5 deg is used to represent the propeller side force.

Simulation for IMO Standards for Ship Maneuverability

2. The IMO Standards for Ship Maneuverability were used as the simulation criteria for identifying IMO standard ships. Ships satisfying all four criteria are defined as IMO class ships, whereas those ships that do not satisfy one or more of the criteria are defined as non-IMO class ships.

- Turning circle: Figure 8*a* shows the results of the simulation of the turning circle test. From this simulation we calculated that the tactical diameter of the ship is 1,523 m, 4.44 times the ship length, which is 343 m. This tactical diameter is much less than the required IMO criterion, which is five times the ship length. The advance is 1,119 m or 3.26 times the ship length. This value is also much less than the IMO criterion of 4.5 times the ship length. Therefore, we concluded that the ship satisfied the IMO criteria of the turning circle test.
- Zigzag test: Figure 8*b* shows the result of the simulation for the 20–20 zigzag test. From this simulation, we can easily determine that the first overshoot is 9.68 deg, much less than the 25 deg of the IMO criteria. Figure 8*c* shows the result of the simulation for the 10–10 zigzag test. From this simulation we can see that the first overshoot is 6.59 deg, and the second overshoot is 14.63 deg. Both of these are much less than the values required by

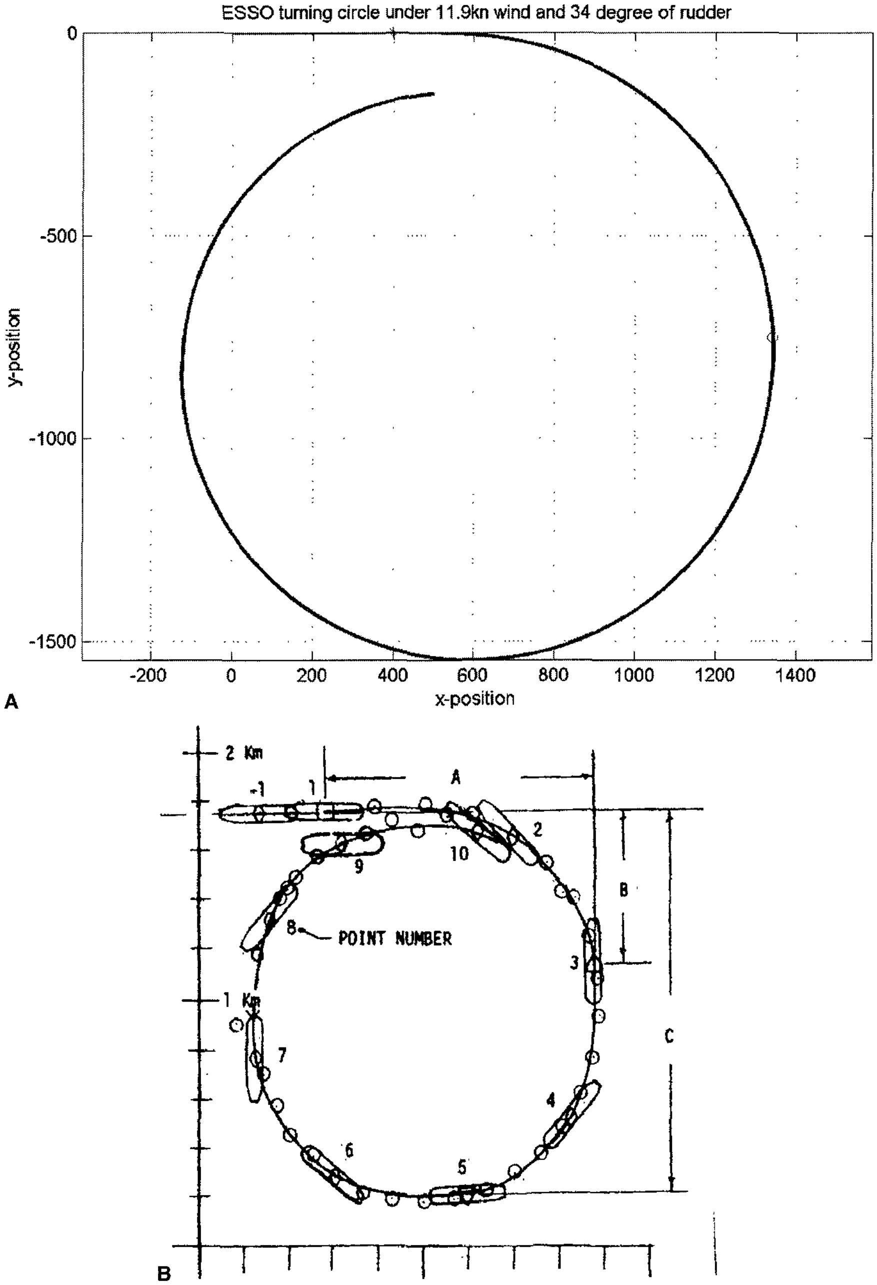

Fig. 7 (A) *Esso Osaka* turning circle comparison. (B) Real trial (Crane 1979a, 1979b)

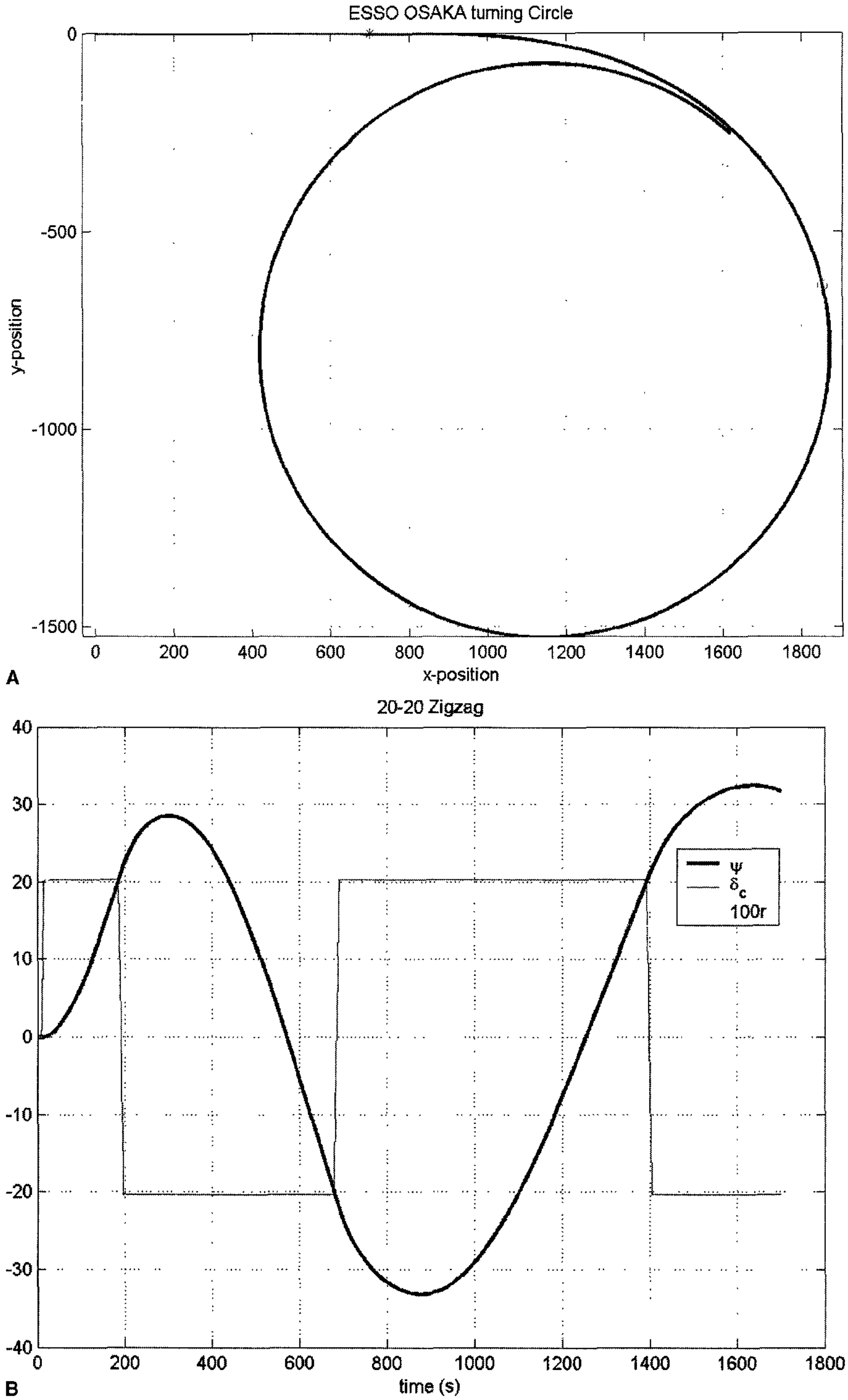

Fig. 8 (A) *Esso Osaka* turning circle course. (B) *Esso Osaka* 20/20 zigzag course

the IMO criteria. Thus, we decided that the ship also satisfies this IMO requirement.

- Initial turning test. Figure 8*d* shows the results of the simulation of the initial turning tests. From this simulation we found that the distance the ship traveled was 669 m, or 1.95 times the ship length. This distance is much less than the requirement of the IMO criterion, which is 2.5 times the ship length. Therefore, we conclude that the ship satisfied the IMO initial turning test criteria.
- Full astern stop. Figure 8*e* shows the results of the simulations for full astern stop. From this simulation we found that the distance the ship traveled was 3,030 m or 8.83 times the ship length. This value is much less than the requirement of the IMO criteria, which is 15 times the ship length. Our conclusion was that the ship satisfied the IMO full astern stopping test criteria. If the starting speed were at full speed, the length could be more than 9 times the ship length.

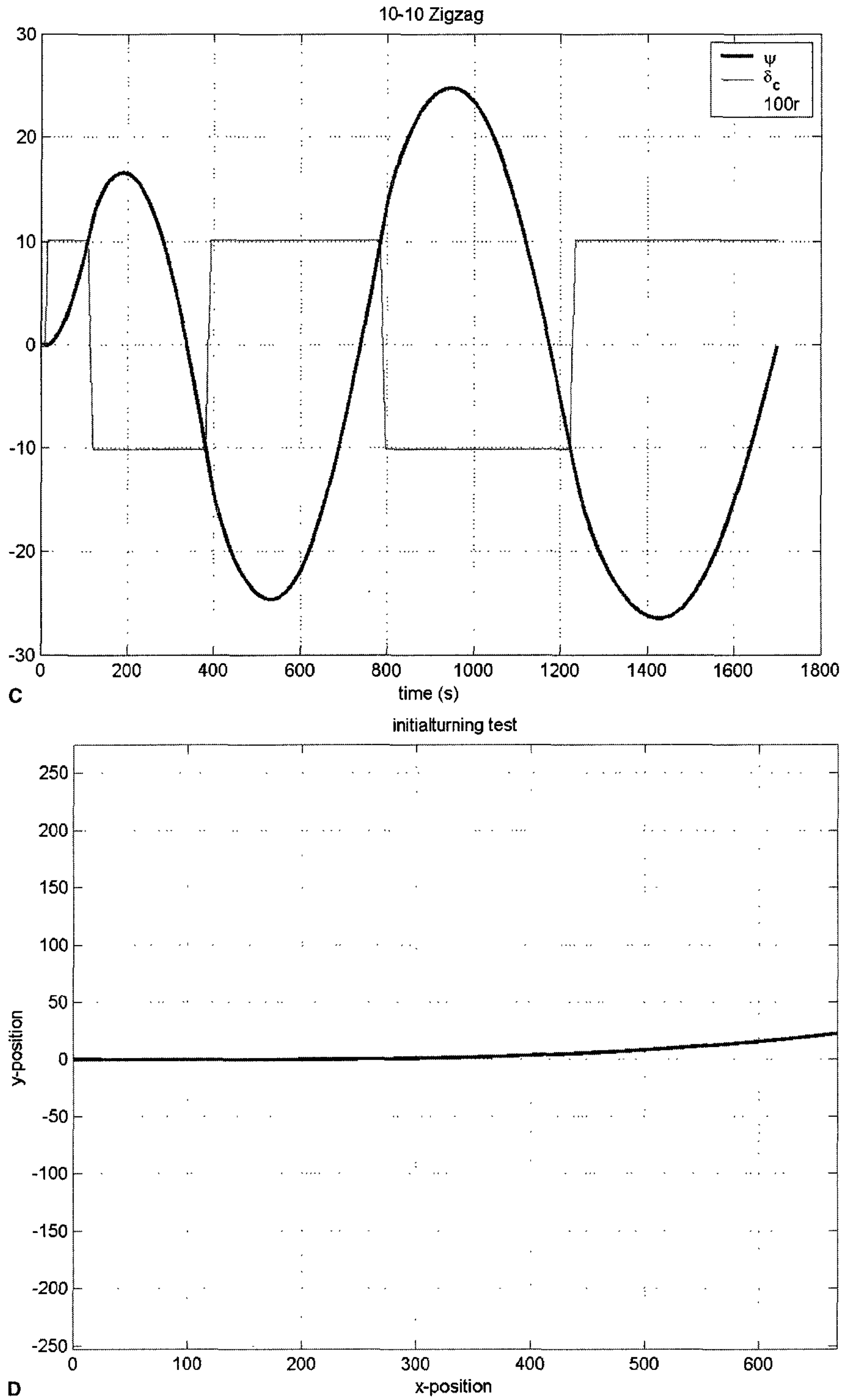

Fig. 8 *(Continued)* (C) *Esso Osaka* 10/10 zigzag course. (D) *Esso Osaka* initial turning course.

As a result, we can claim that *Esso Osaka* is an IMO class ship.

In the same way that an IMO class ship has been identified, so could also a non-IMO ship be identified. A Mariner class ship with the governing equations given by Chislett and Strom-Tejsen (1965) is selected as an example for validation. This ship's length is 160.93 m. According to the IMO criteria, the tactical diameter should not exceed five times the ship length, nearly 805 m, which is less than the simulation result of the Mariner, 1,100 m, in Fig. 8*f*. This particular Mariner ship is identified as a ship not satisfying the current IMO criteria for the turning circle test. That is to say, we can conclude that this particular Mariner class ship is a non-IMO Standard ship for maneuverability. However, with such modifications as changing its rudder size, it might satisfy the IMO Standards.

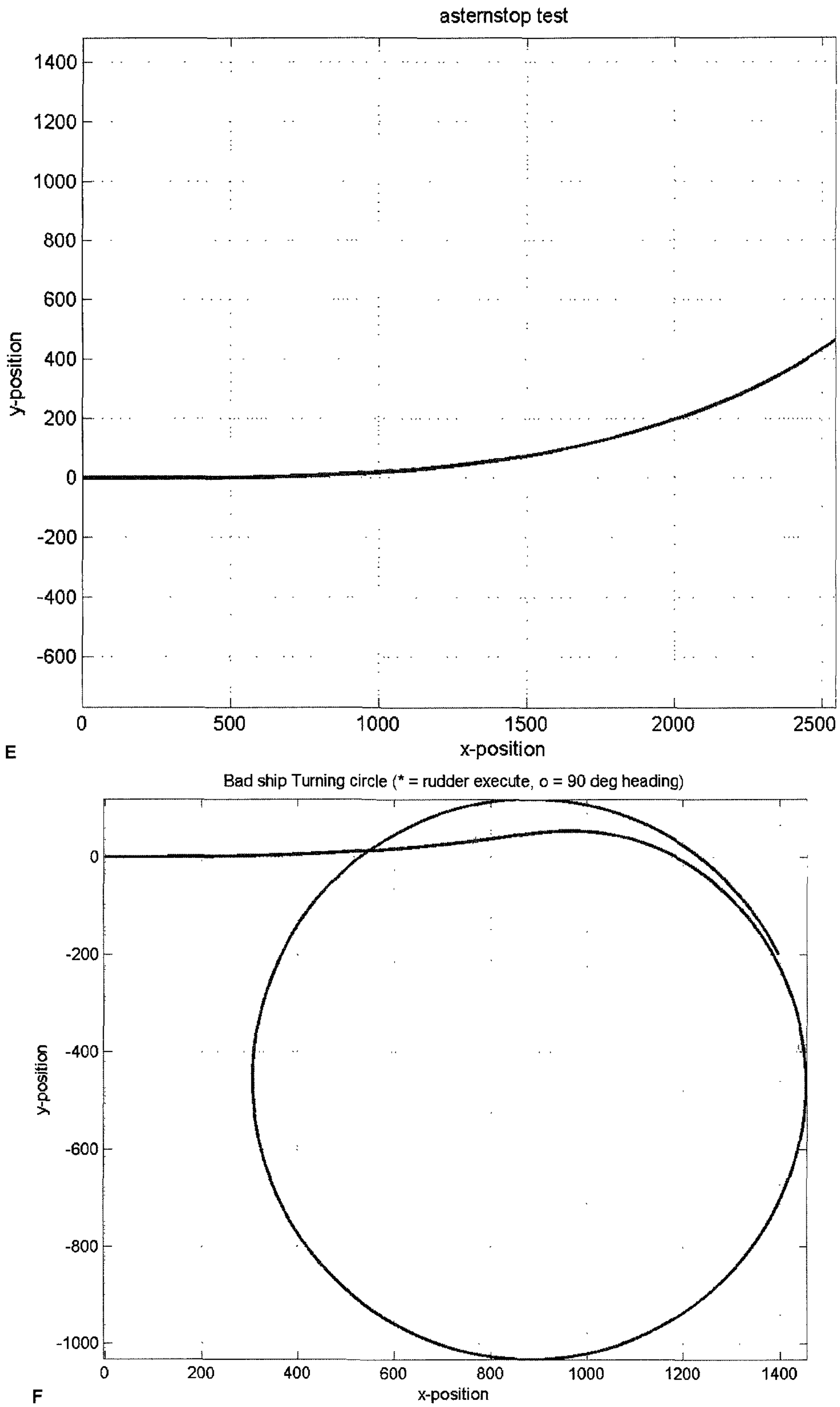

Fig. 8 *(Continued)* (E) *Esso Osaka* full astern stopping course. (F) Mariner class cruise turning circle course

Simulations for safe entrance into harbor

One can see, as in Fig. 6, that a tanker normally sails straight into the harbor following the navigation channel. At a specific location, she starts turning. The initial conditions for the ship are given in Table 2. During the simulation, the *Esso Osaka* was required to turn 1.2 (rad) into the harbor under the combined conditions of wind and current. The wind speed chosen for the simulation was 30 knots coming from −30 deg and the current speed was 1 knot also coming from 30 deg.

Table 2 Initial value of the *Esso Osaka*

u	4 m/s
ν	0 m/s
ψ	0 rad
r	0 rad/s
Pre-turn time	1 s

Figure 9*a* shows the ship course as a result of the simulation for the ship entering in the harbor. In this case, the ship sails straight only just in the very first second and enters in the regular navigational channel, as shown in Fig. 5. The heading angle obtained in simulation is given in Fig. 9*b*. The yawing rate calculated in the simulation is given in Fig. 9*c*. The rudder angle obtained in simulation is given in Fig. 9*d*. The travel lengths in x and y direction of the simulation are shown in Fig. 9*e* and Fig. 9*f*. The speeds of u and v of the simulation are shown in Fig. 9 *g* and *h*.

From the pre-turning analysis, we know that the angle the ship should turn is 1.2 (rad), shown in Fig. 9*b*. From the result of simulation, one can see that the heading angle is about 1.24 (rad) after the 300th second. If we take the 300th second as a measure, the error is about 3.3% in turning angle. The error is observed to decrease as the simulation time increases.

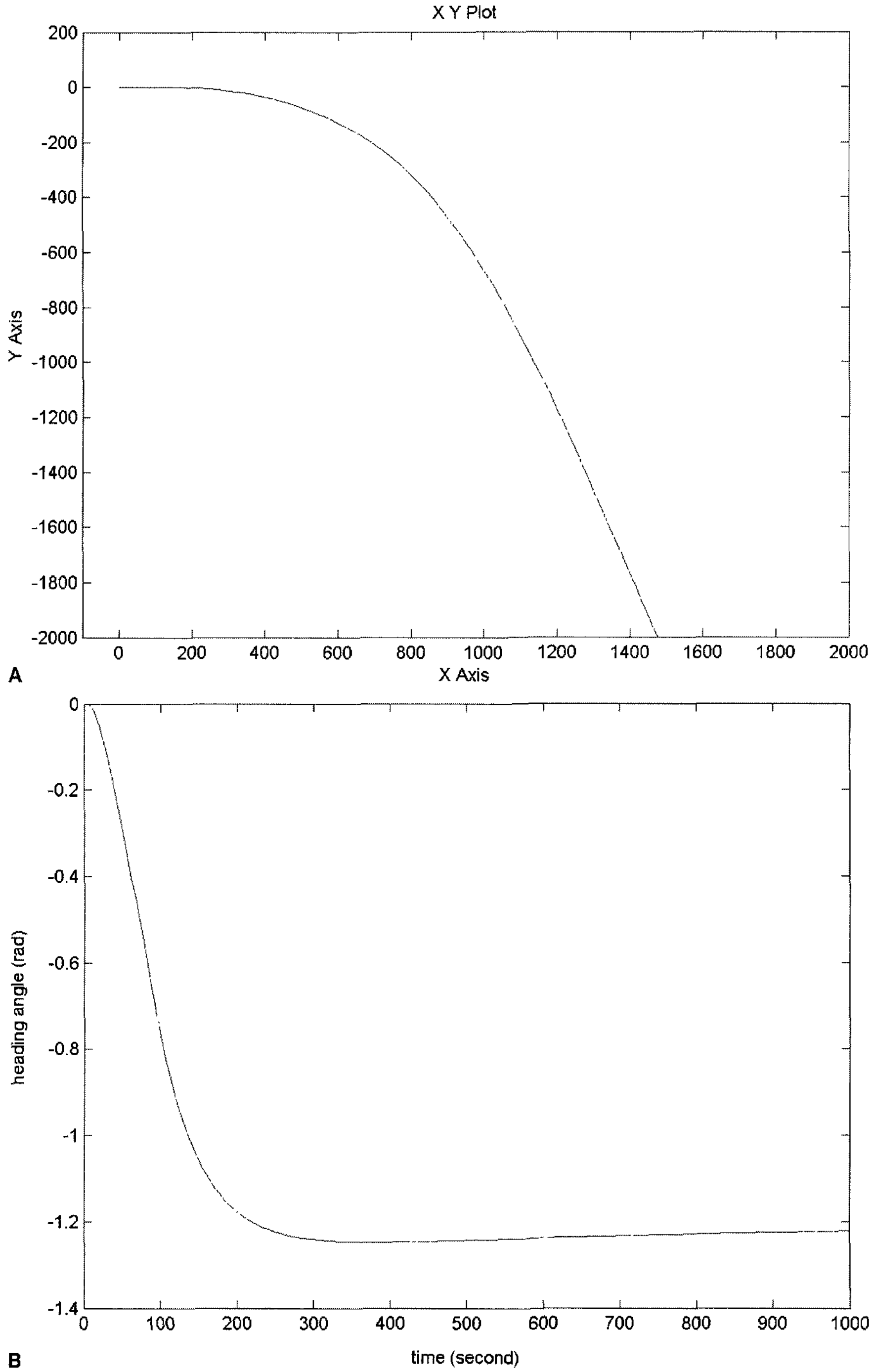

Fig. 9 (A) Course of entering harbor at an initial required angle of 1.2 (rad). (B) Heading angle: ψ during the course

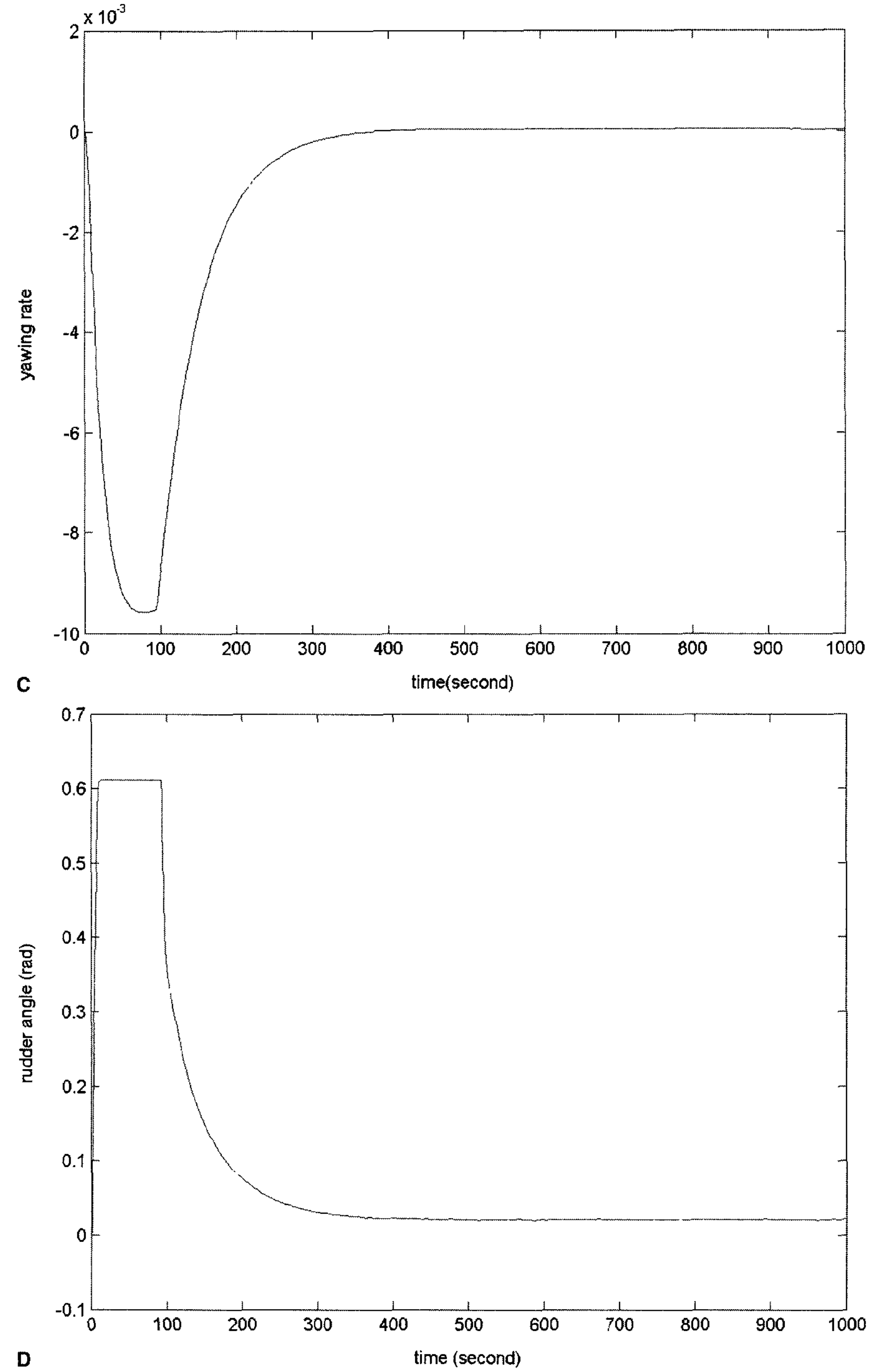

Fig. 9 *(Continued)* (C) Yawing speed: r during the course. (D) Rudder angle: δ during the course

Simulation with tug assistance

In this section, one escort tug is included in the simulation. Figure 10a shows the breaking force and steering force that this tug can provide to the tanker when it is turning under the conditions given in Table 1 (see Fig. 7 a and b). Figure 10b shows the result of *Esso Osaka* turning circle with escort tug assistance. The tactical diameter in Fig. 10b is 1,540 m here compared with 1,564 m in Fig. 7a. With the tug's assistance, the tanker can now maintain an improved maneuvering performance and possibly increase its safety in bad weather. Through simulation, the number of escort tugs necessary for safe maneuvering can be estimated.

As stated in the modeling section, besides the assistance to wind and wave effects, the tug assistances to enhance tanker performance in calm water conditions are also considered.

Figures 10 c and d show the results of a single escort tug assisting *Esso Osaka*. One can observe that all values required by IMO significantly decrease. In addition, multiple tug assistances are evaluated, and the results are shown in

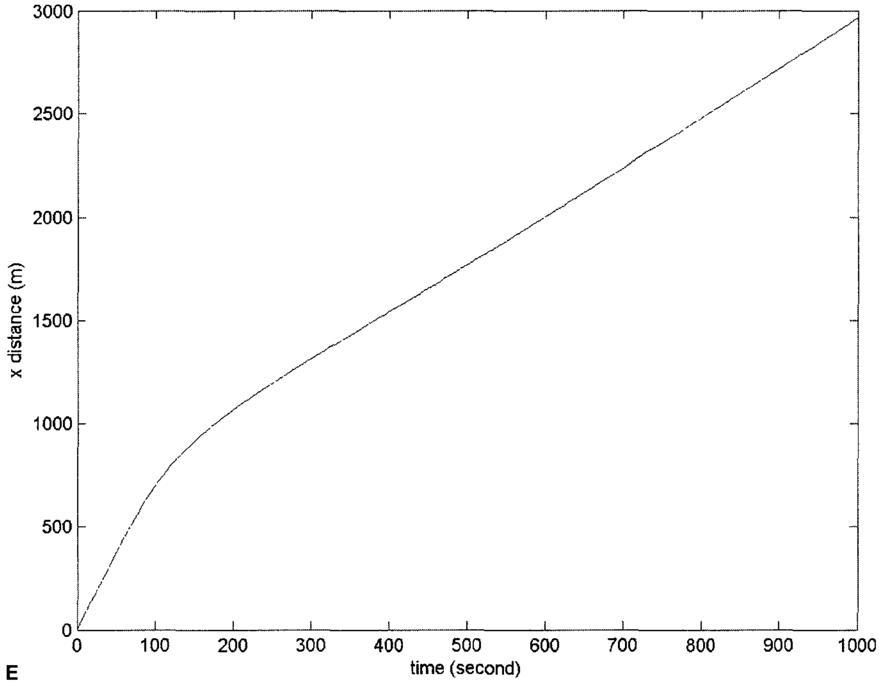

E

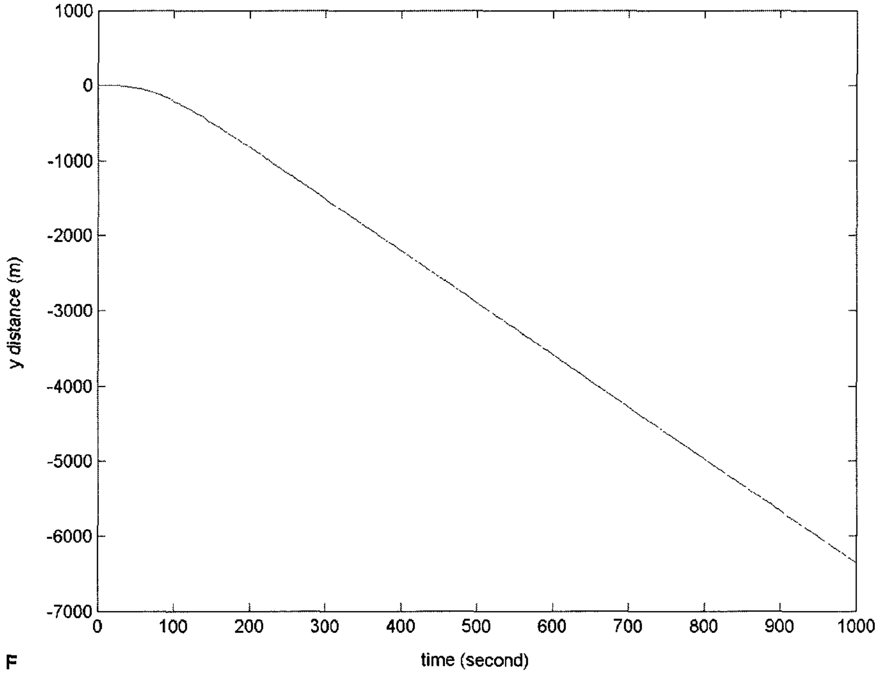

F

Fig. 9 *(Continued)* (E) *x* distance during the course. (F) *y* distance during the course

Table 3. The increment in assistance by using an additional tug is observed to be less than the assistance or improvements provided by the first one. This could be the result of the linear increase of the tug forces and moments while the hydrodynamic forces and moments increase nonlinearly. The incremental assistance by additional tugs is quantified for wind and wave conditions and is discussed below.

Harbor entrance limit conditions

To study the simulation under the wind and current conditions systematically, a pair of wind speed and current speed values are selected. The simulation by UBCManeuver then suggested a safe entrance in the harbor area or a ship movement outside of the assigned navigation channel area. If the simulation suggests a ship movement outside the assigned area, the combination of wind and current is considered an "unsafe" condition on the plot of wind and current space in Fig. 11*a*. This point is marked as an "unsafe" region. A ceiling of safe operation in this space is obtained as a band labeled as "unknown." The maximum wind condition measured around Vancouver harbor is 65 knots from −30 deg and the strength of tidal current is around 5.5 knots (−30 deg). In Fig. 11*a*, consequently, the upper limits of wind and current

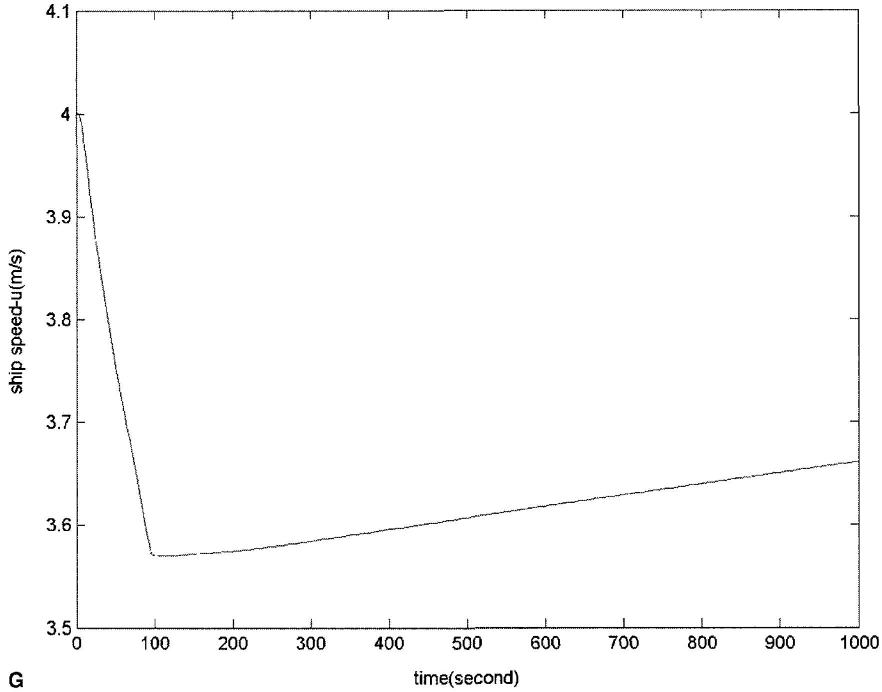

G

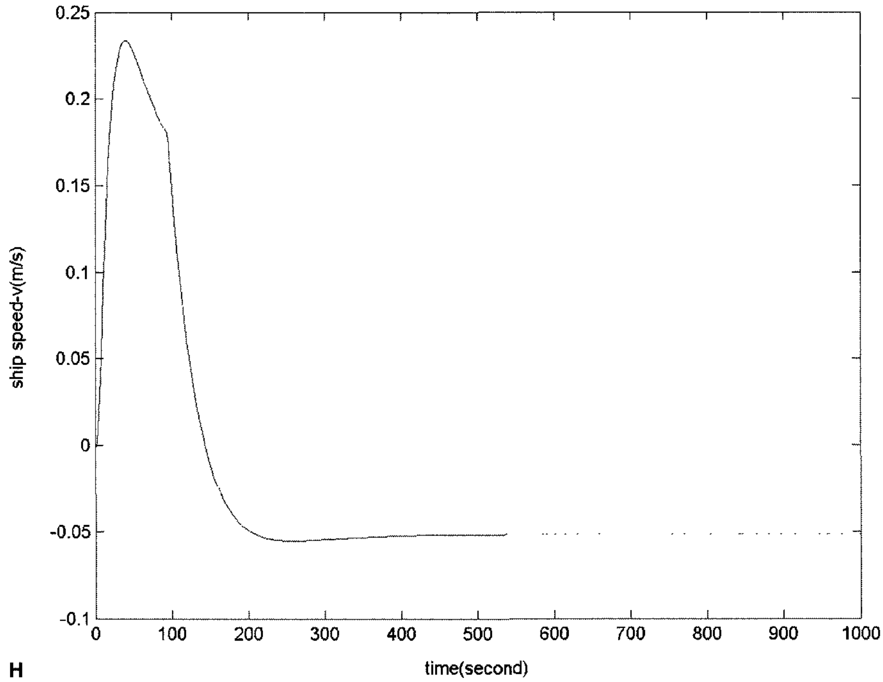

H

Fig. 9 *(Continued)* (G) Surge velocity *u* during the course. (H) Sway velocity *v* during the course

speeds are selected somewhat higher than maximum data values as 80 knots and 6 knots as the scales of vertical and horizontal axes. Figure 11*a* shows three distinct areas that are labeled as safe, unsafe, and unknown. One can see that the "unknown" area covers a band where the current speed is in the interval from 1.8 knots to 2.4 knots while wind speed is 0 knots. The unknown band can be defined as the limit of the safe operation for a particular ship. In order to obtain more precise results, one needs to take more combinations of current and wind effects in the unknown area to narrow down the width of this band. Figure 11*b* is obtained after the usage of a finer mesh for the combination of wind and current speeds, a zoom-in area where wind speed is 0 knots to 20 knots and current speed is 1.75 knots to 1.95 knots. The limit of the safe operation is 1.825 knots to 1.85 knots of current speed compared with 1.8 knots to 2.4 knots in Fig. 11*a* while the wind speed is 0 knots.

The same simulation study is done with an escort tug. With a tug's assistance, the tanker can maintain a better performance and the ceiling of safe operation is seen to increase in bad weather. Figures 11 *c* and *d* show that such a tug can provide significant assistance to ship course keeping and in-

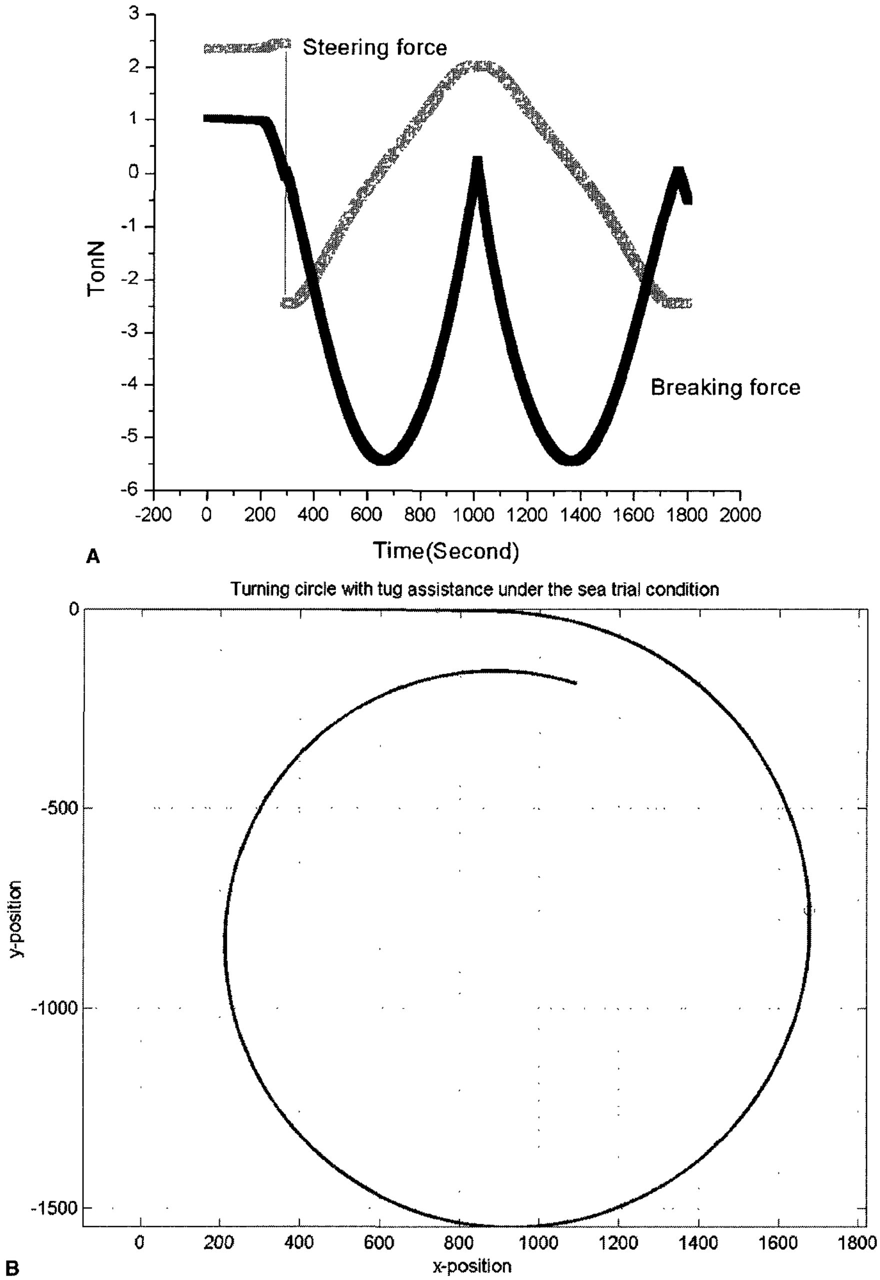

Fig. 10 (A) Breaking force and steering force for *Esso Osaka* turning circle. (B) *Esso Osaka* turning circle with escort tug assistance to counter external effects

creases the maneuvering performance of a ship at the entrance to a harbor. The limit of the safe operation of a ship with an escort tug linked to the bow of the tanker increases to 2.1 knots of current speed while the wind speed is 0 knots, and for the tanker with an escort tug connected to the stern the ceiling is seen to increase to 2.225 knots compared with 1.85 knots without tug assistance. These results are shown in Fig. 11*b*. Considering the measure of improvement in maneuvering proportional to the percent increase in the safe areas in Figs. 11 *a* and *c*, one can claim that the possibility of safe operation increases about 25% with one escort tug connected at the bow and 42% with one escort tug connected at the stern. The basis of comparison is the area under the ceiling band for the results obtained without the help by escort tug under the same condition. Figure 11*e* shows the result obtained with the simulation for the tanker with two stern-connected escort tugs. In this case the possibility for safe entrance increases about 75% compared to the operation without the help of an escort tug.

Generally speaking, the possibilities of safe entrance into Vancouver Harbor with and without escort tug assistance can be obtained through Figs. 11 *a* and *e*. From these results of the simulation, it is easy to conjecture that the current effect is much stronger than the wind effect for the *Esso Osaka* tanker in Vancouver Harbor. The simulations suggest that it will be difficult for *Esso Osaka* to enter into Vancouver Harbor under nearly two thirds of the current conditions even without wind effects. On the other hand, she can enter

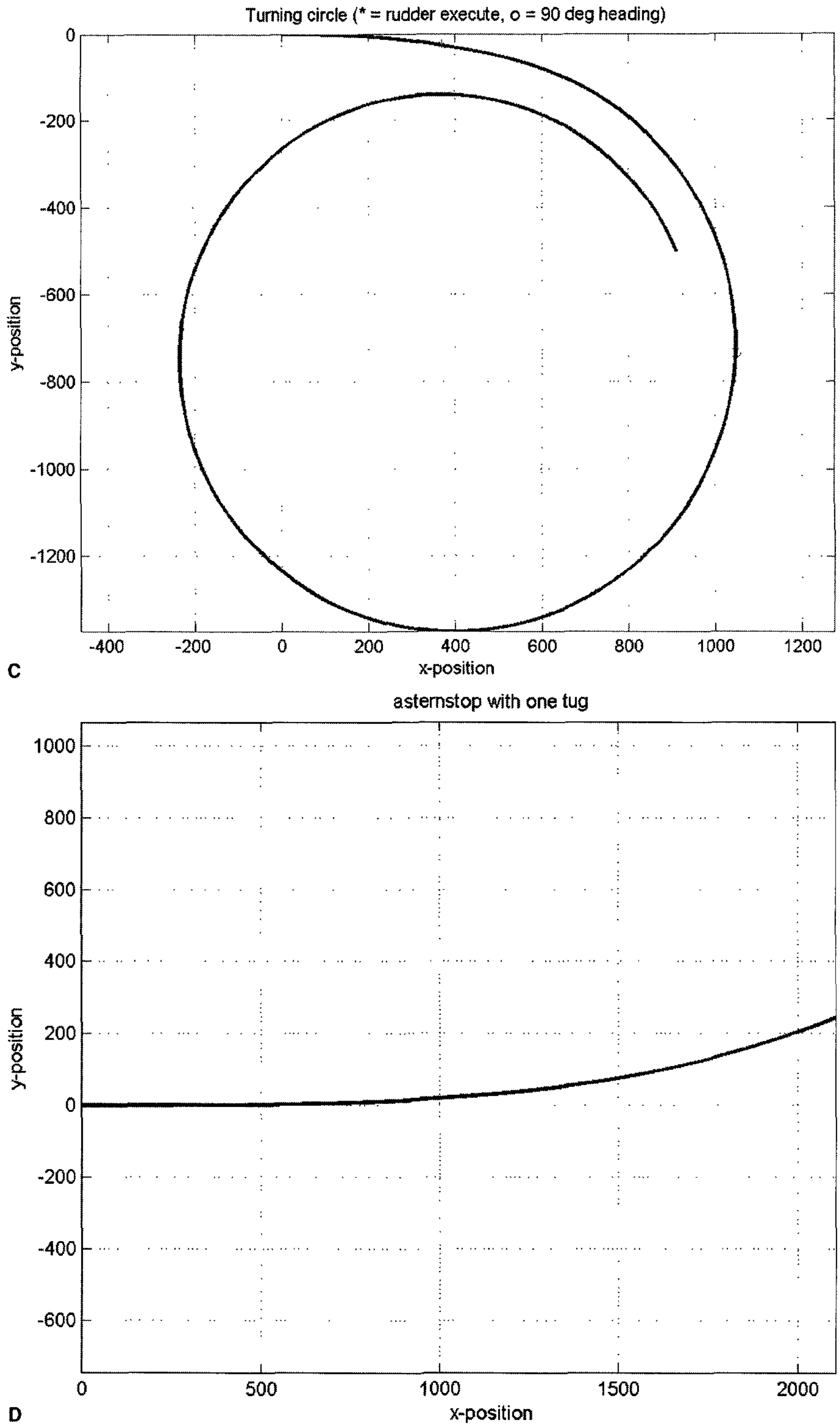

Fig. 10 *(Continued)* (C) *Esso Osaka* turning circle with general escort tug assistance. (D) *Esso Osaka*, full astern stopping with general escort tug assistance

the harbor under all wind conditions if there are no currents in the harbor.

Conclusion

After all above simulation studies, some general conclusions could be drawn:

1. The validation of the mathematical simulation with the sea trial of 1977 suggests good agreement with test results. The differences between the experimental and numerical lengths for IMO requirements were less than 2%. One can claim that UBCManeuver is a satisfactory program for evaluating tanker maneuvering performance.

Table 3 Tug assistance performance for IMO standard tests

Test	Values	IMO Value	No Tug	One Tug	Two Tugs
Turning circle test	Tactical diameter	5 L	1,523 m (4.44 L)	1,294 m (3.78 L)	1,116 m (3.26 L)
	Difference with no tug			15.1%	26.7%
20/20 Zigzag test	First overshoot	25 deg	9.68 deg	8.00 deg	7.29 deg
	Difference with no tug			17.4%	24.7%
Initial turning test	Travel length	2.5 L	669 m (1.95 L)	511 m (1.49 L)	418 m (1.22 L)
	Difference with no tug			23.6%	37.5%
Full astern stopping test	Travel length	15 L	3,030 m (8.83 L)	2,341 m (6.83 L)	1,937 m (5.65 L)
	Difference with no tug			22.74%	36.7%

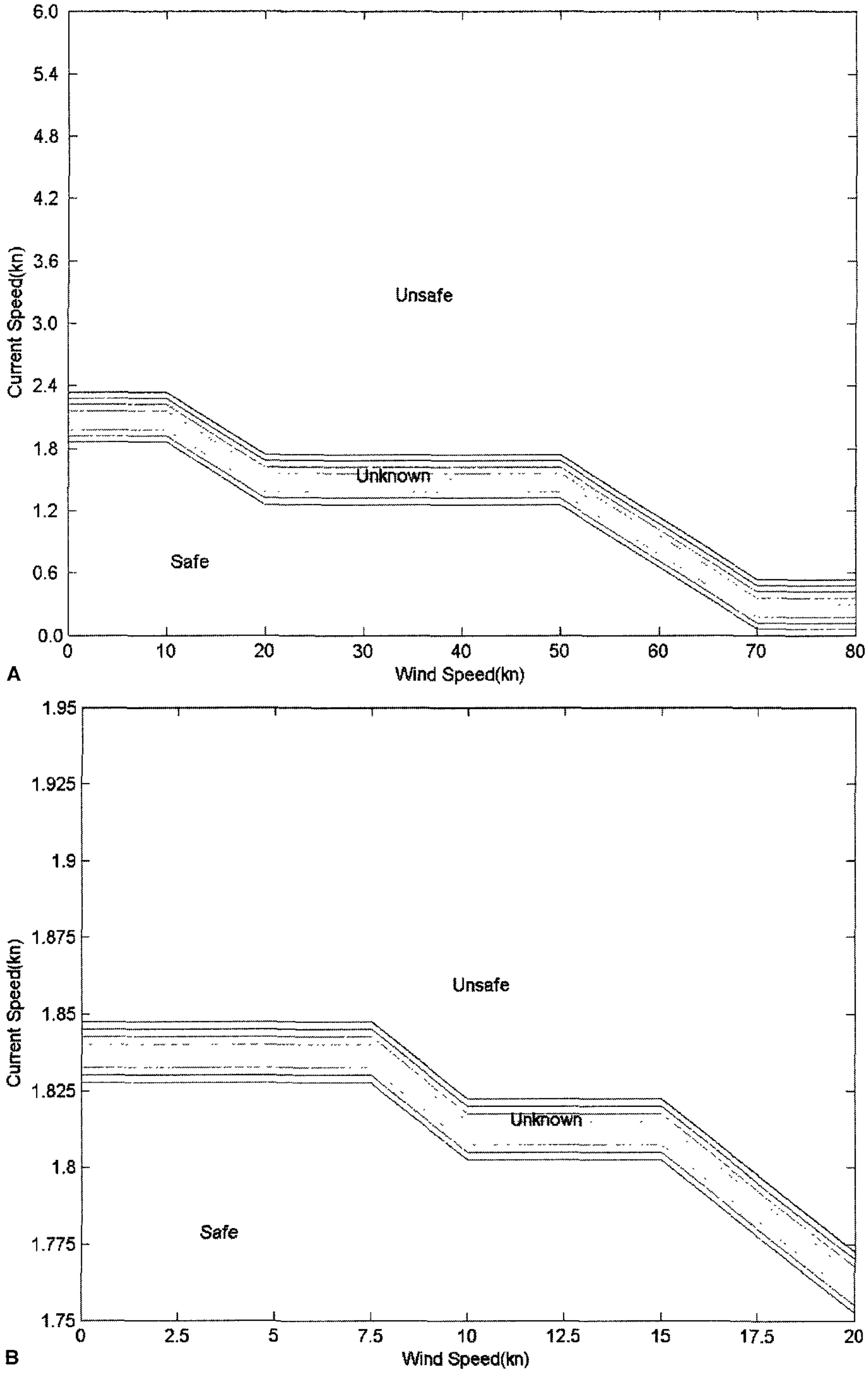

Fig. 11 (A) Possibility of *Esso Osaka* turning into Vancouver harbor. (B) Zoom-in result of possibility of *Esso Osaka* turning into the harbor without tug assistance

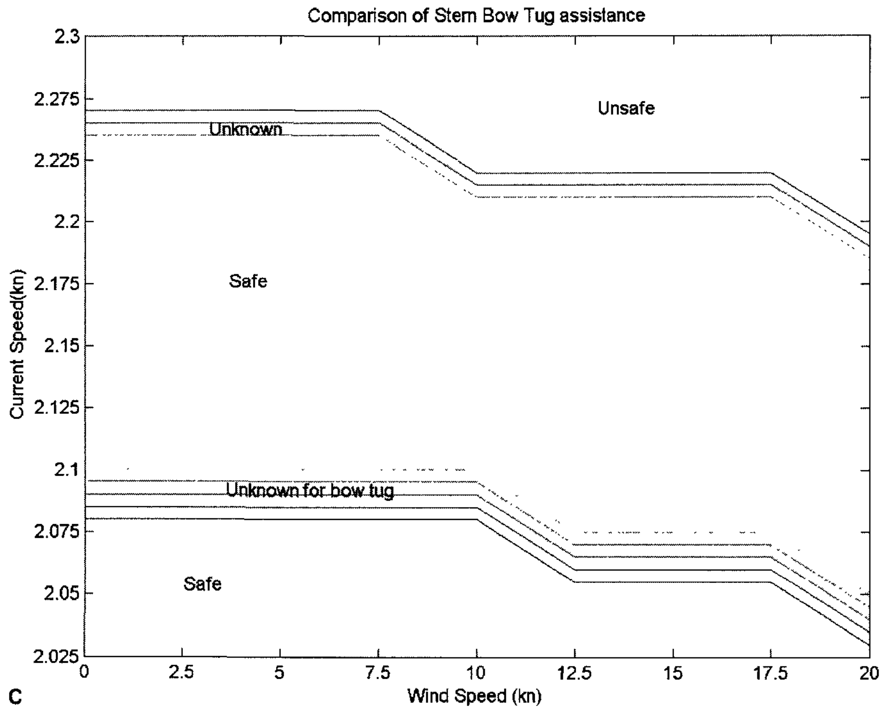

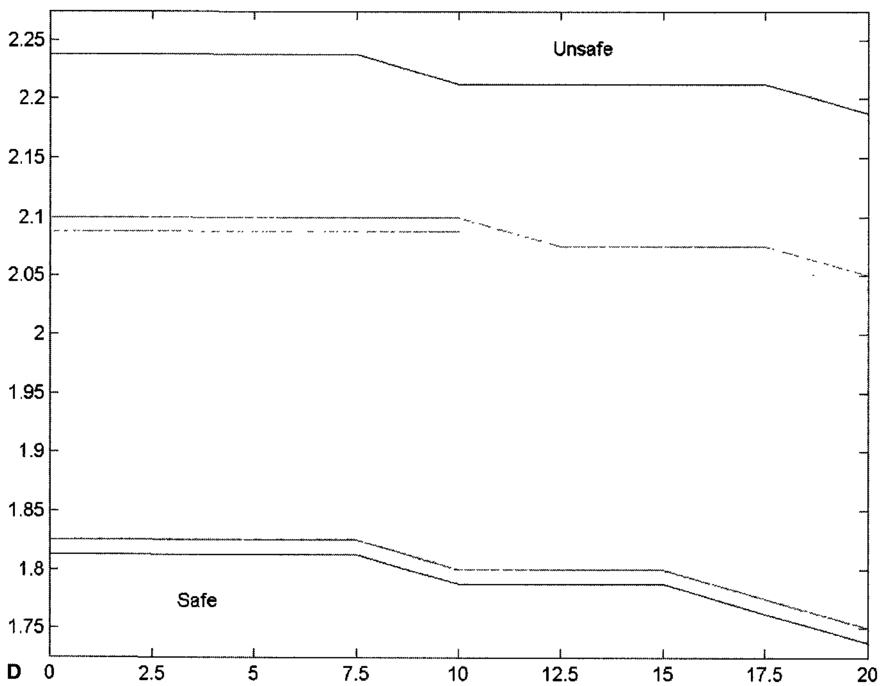

Fig. 11 *(Continued)* (C) Possibility of *Esso Osaka* turning into the harbor with tug assistance. (D) Comparison of possibility of *Esso Osaka* turning into the harbor with and without tug assistance.

2. Concerning the ship simulation test to establish if a tanker meets the current IMO Standards, one can claim that UBCManeuver can predict the ship maneuvering performance to see if the tanker meets the current IMO Standards. UBCManeuver was also able to identify a ship that did not meet these criteria.
3. It was shown that various combinations of escort tug performances with tankers can be successfully simulated with UBCManeuver. A measure of tug performance enhancement for a tanker is provided.
4. Concerning the ship course-keeping performance, with the help of the PID control algorithm, under regular bad weather around Vancouver Harbor, the error between required turning angle value and simulated result is 3.3%.
5. The safe entrance in Vancouver Harbor under wind and current conditions was studied. The simulation suggests that the current effect is more important and severe than the wind effects for this harbor. The tug assistance that was simulated proved to be significant, improving the safety at harbor entrance by about 40%.

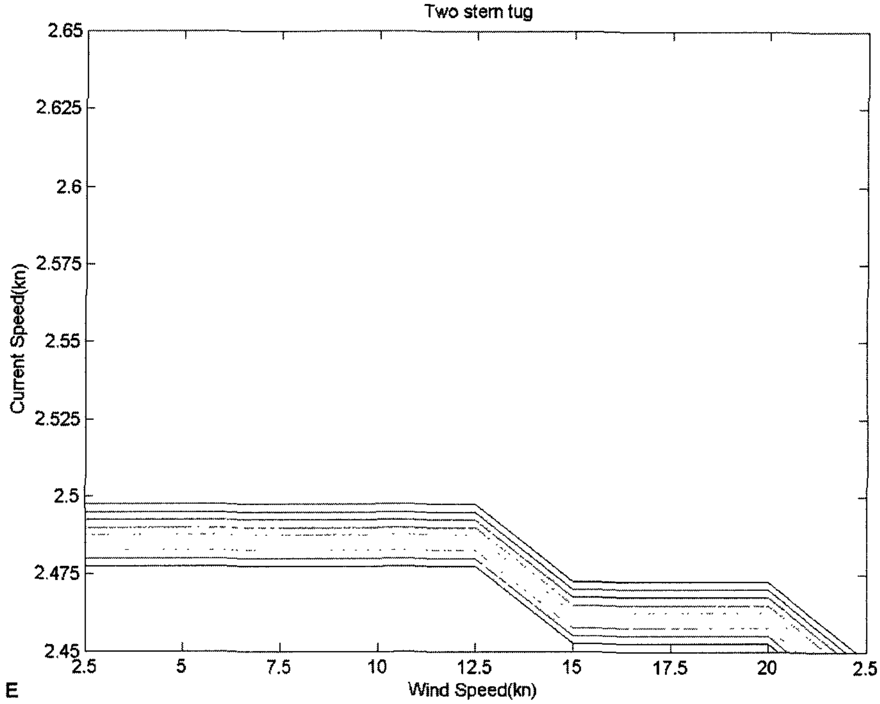

Fig. 11 *(Continued)* (E) Possibility of *Esso Osaka* turning into the harbor with assistance from two stern escort tugs

6. The simulation to the same problem has been done with another simulation software system named AutoLev, which is suitable for any rigid body motion problem, and similar results have been obtained. The difference between the results obtained with the two simulation programs was less than 0.05%. The details of the work with AutoLev will be reported separately.

Acknowledgments

The authors deeply appreciate Dr. Kim of KRISO for providing the tanker test data, especially some unpublished data; the Canadian Hydrographic Service (CHS) for providing the current data; and Environment Canada for providing wind data around Vancouver Harbor.

The authors would also like to thank Mr. Alex C. Landsburg, Maritime Administration program manager of the Department of Transport in the United States and chairman of Panel H-10 (ship controllability) of the Society of Naval Architects and Marine Engineers, for explaining some important points.

References

Baquero, A. 1982 *An Analysis of the Behavior of Ships under Steering—Hydrodynamics and Design Feature*, EI Pardo Tanker Report No. 66, Madrid, Spain.

Chislett, M. S., and Strom-Tejsen, J. 1965 *Planar Motion Mechanism Tests and Full-Scale Steering and Maneuvering Predictions for Mariner Class Vessel*, Technical Report Hy-6, Hydro- and Aerodynamics Laboratory, Copenhagen, Demark.

Crane, C. L., Jr. 1973 Maneuvering safety of large tankers: stopping turning, and speed selection, *Transactions of the Society of Naval Architects and Marine Engineers,* **81**, 213–243.

Crane, C. L., Jr. 1979a *Maneuvering Trials of the 278,000 DWT Esso Osaka in Shallow and Deep Water*, Exxon International Company Report EII.4TM.79.

Crane, C. L., Jr. 1979b Maneuvering trials of the 278,000 DWT tanker in shallow and deep waters, *Transactions of the Society of Naval Architects and Marine Engineers*, **87**, 251–283.

Daidola, J. C., Lundy, W., and Barr, R. 2002 Evolution of IMO standard for maneuverability, *Transactions of the Society of Naval Architects and Marine Engineers*, **110**, 395–411.

Djouani, K., and Hamam, Y. 1996 Feedback optimal neural network controller for dynamic systems—a ship maneuvering example, *Mathematics and Computers in Simulation*, **41**, 117–127.

Doerffer, J. W. 1980 Standardization of ship maneuvering characteristics, *Computer Applications in Shipping and Shipbuilding*, **8**, 163–169.

Eda, H., Falls, R., and Walden, D. A. 1979 Ship maneuvering safety studies, *Transactions of the Society of Naval Architects and Marine Engineers*, **87**, 229–250.

Gray, W. O., Waters, J. K., Blume, A. L., and Landsburg, A. C. 2003 Channel design and vessel maneuverability: next steps, Marine Technology, **40**, 2, 93–105.

Guedes Soares, C., Francisco, R. A., Moreira, L., and Laranjinja, M. 2004 Full scale measurements of the manuevering capabilities of fast patrol vessels, Argos class, Marine Technology, **41**, 1, 7–16.

Hasegawa, K., and Sasaki, Y. 1997 Java-based simulation tool for ship maneuvering, *Proceedings*, 4th International Conference on Maneuvering and Control of Marine Vehicles, September, Brijuni, Croatia, 139–144.

IMO, Maritime Safety Committee. 2002 Standards for Ship Maneuverability, Resolution MSC 136 (76), International Maritime Organization, December 4.

ITTC. 2002 Specialist committee report of Proceedings of ITTC 2002, September, Rome, Italy.

Kim, S.Y. 1988 *Development of Maneuverability Prediction Technique*, Korea Institute of Machinery and Materials (KIMM) Report No. UCE.337–1082.D, Dae Jeon, Korea.

Kvam, K., Ohtsu, K., and Fossen, T. I. 2000 Optimal ship maneuvering using Bryson and Ho's time varying LQ controller, *Proceedings*, IFAC MCMC, August, Aalborg, Denmark.

Nomoto, K., Taguchi, T. , Honda, K., and Hirano, S. 1957 On steering qualities of ships: technical report, *International Shipbuilding Progress*, **4**, 35.

OCIMF. 1977 *Prediction of Wind and Current Loads on VLCCs*, The Oil Companies International Marine Forum.

Palomares, M. 1994 The role of IMO in setting maneuvering standards, *Proceedings*, IFAC MCMC, September, Southampton, UK.

Ratcliff, A. 2004 *A Study of Hydrodynamic Performance of Voith-Schneider Propelled Escort Tugs,* M.A.Sc thesis, Department of Mechanical Engineering, University of British Columbia, Vancouver, Canada, November.

Van Berlekon, W. B., Trangardh, P., and Dellhag, A. 1974 Large tankers—wind coefficients and speed loss due to wind and sea, Royal Institution of Naval Architects meeting, April 25, London, 41–58.

Von Wagner, B. 1967 Windkrafte an Uberwasserschiffen, *Schiff und Hafen*, **12**, 19 Jahrgang, 894–900 (in German).

Webb, D. W., and Hewlett , J. C. R. 1992 Ship simulation of the Houston ship channel, *Proceedings*, PORTS, vol. 1, 898–911.